# Stokes shift in semi-polar ( $11\bar{2}2$) InGaN/GaN multiple quantum wells

Y. Zhang, R. M. Smith, Y. Hou, B. Xu, Y. Gong, J. Bai, and T. Wang

Citation: Appl. Phys. Lett. **108**, 031108 (2016); doi: 10.1063/1.4940396
View online: http://dx.doi.org/10.1063/1.4940396
View Table of Contents: http://aip.scitation.org/toc/apl/108/3
Published by the American Institute of Physics

**Articles you may be interested in**

Defect reduction in overgrown semi-polar (11-22) GaN on a regularly arrayed micro-rod array template
AIP Advances **6**, 025201 (2016); 10.1063/1.4941444

(11-22) semipolar InGaN emitters from green to amber on overgrown GaN on micro-rod templates
Applied Physics Letters **107**, 261103 (2015); 10.1063/1.4939132

Microstructure investigation of semi-polar (11-22) GaN overgrown on differently designed micro-rod array templates
Applied Physics Letters **109**, 241906 (2016); 10.1063/1.4972403

Band parameters for nitrogen-containing semiconductors
Journal of Applied Physics **94**, 3675 (2003); 10.1063/1.1600519

Radiative recombination mechanisms in polar and non-polar InGaN/GaN quantum well LED structures
Applied Physics Letters **109**, 151110 (2016); 10.1063/1.4964842

Semi-polar (11-22) AlGaN on overgrown GaN on micro-rod templates: Simultaneous management of crystal quality improvement and cracking issue
Applied Physics Letters **110**, 082103 (2017); 10.1063/1.4977094

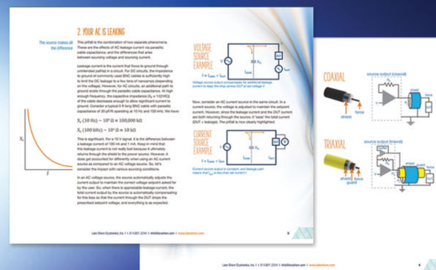

5 Electronic Measurement Pitfalls to Avoid
Get the whitepaper

# Stokes shift in semi-polar ($11\bar{2}2$) InGaN/GaN multiple quantum wells

Y. Zhang, R. M. Smith, Y. Hou, B. Xu, Y. Gong, J. Bai, and T. Wang[a)]
*Department of Electronic and Electrical Engineering, University of Sheffield, Mappin Street, Sheffield S1 3JD, United Kingdom*

(Received 3 December 2015; accepted 11 January 2016; published online 20 January 2016)

The mechanism for the large Stokes Shifts of InGaN/GaN structures is under debate. Here, we report a systematic study on the Stokes shift of semi-polar ($11\bar{2}2$) InGaN/GaN multiple quantum wells (MQWs) with a wide spectral range from green (490 nm) to yellow (590 nm) by means of both photoluminescence excitation and time resolved PL measurements in comparison with their *c*-plane counterparts. The semi-polar samples exhibit a lower Stokes shift than their *c*-plane counterparts, although they show stronger localization effect than their *c*-plane counterparts. In the long wavelength region, the Stokes shift of the semi-polar MQWs shows a linear relationship with emission energy, but with a smaller gradient compared with their *c*-plane counterparts. The time-resolved PL measurements confirm a significant reduction in piezoelectric field of the semi-polar samples compared with the *c*-plane counterparts. It is suggested that the piezoelectric field induced polarization is the major mechanism for causing the large Stokes shift. The presented results contribute to better understanding of the long standing issue on the mechanism for the large Stokes shift. © *2016 AIP Publishing LLC*. [http://dx.doi.org/10.1063/1.4940396]

Tremendous progress has been made in the field of III-nitride optoelectronics grown on (0001) sapphire within last two decades, represented by high brightness InGaN/GaN based blue emitters, leading to three Nobel Prize Winners in 2014. However, there are still great challenges to be overcome to improve the optical performance of InGaN/GaN based structures when moving towards the longer wavelength, such as the green and yellow spectral region.[1] Due to the large lattice mismatch between InN and GaN, strain-induced piezoelectric fields along the *c*-direction are generated across the InGaN/GaN based active layer, causing the well-known quantum-confined Stark effect (QCSE). This separates the electron and hole wavefunctions in opposite directions, leading to a great decrease in radiative transition rate and thus optical quantum efficiency. On the other hand, the solid immiscibility between InN and GaN makes it difficult to grow InGaN with high indium content, which is necessary for the emitters with long emission wavelengths.[2] To circumvent the problems caused by the internal electric fields, a promising solution is to grow InGaN/GaN structures along either non-polar or semi-polar orientation in order to eliminate or reduce the polarization fields.[3] Furthermore, in comparison with either polar or non-polar planes, semi-polar ($11\bar{2}2$) GaN exhibits a higher indium incorporation ability as a result of a much lower indium chemical potential on its surface than either the non-polar or polar surface.[4] In this case, InGaN grown along the ($11\bar{2}2$) direction can accommodate more indium atoms under same growth conditions, potentially allowing us to obtain InGaN layers with high indium content, which is essential for green and yellow emitters.

The difference between emission energy and absorption energy in semiconductor materials, known as Stokes shift, can be measured by photoluminescence excitation (PLE) measurements. Up until now, the issue on the large Stokes shift in *c*-plane InGaN/GaN structures (polar) has been studied extensively,[5–10] but the mechanisms for the large Stokes shifts are controversial, as two major issues, both QCSE and indium segregation induced localization effects existing in *c*-plane InGaN/GaN structures simultaneously, cannot be clearly separated. Furthermore, it is very difficult to achieve emission with long wavelengths using *c*-plane InGaN/GaN structures. Therefore, it is a great challenge to draw a clear and universal conclusion for the cause of the large Stokes shifts of InGaN/GaN structures. In order to address the challenging issue, it is necessary to investigate the Stokes-shift of semi-polar InGaN/GaN structures with high crystal quality, and also compare with *c*-plane InGaN/GaN structures. (A non-polar InGaN/GaN structure would be ideal, but as mentioned above it would be almost impossible to achieve emission with long wavelengths using non-polar InGaN/GaN structures. Therefore, it could be difficult to draw a universal conclusion if we would use non-polar InGaN/GaN structures).

However, owing to greatly technological challenges in growing high quality semi-polar ($11\bar{2}2$) GaN, there is almost an absence of reports on the study of the Stokes shift of semi-polar ($11\bar{2}2$) InGaN/GaN multiple quantum well (MQW) structures. Recently, we have developed a number of cost-effective approaches to the overgrowth of semi-polar GaN.[11–13] On such high crystal quality semi-polar GaN, our group has grown a number of semi-polar ($11\bar{2}2$) InGaN/GaN MQW samples with high optical performance by metalorganic chemical vapor deposition (MOCVD), allowing us to systematically investigate the optical properties of semi-polar InGaN/GaN MQWs. In this letter, we report a systematic study of the Stokes shifts of a series of high-quality semi-polar ($11\bar{2}2$) InGaN/GaN MQWs with a wide spectral range by both PLE and time resolved PL measurements, and then compare with *c*-plane InGaN/GaN MQWs. Although the semi-poplar InGaN/GaN MQWs demonstrate deeper

[a)]Author to whom correspondence should be addressed. Electronic mail: t.wang@sheffield.ac.uk

 © 2016 AIP Publishing LLC

localized states than the *c*-plane counterparts over a wide spectral range, the Stokes-shifts of the semi-poplar InGaN/GaN MQWs are generally much smaller than those of the *c*-plane counterparts. This clearly demonstrates the piezoelectric field induced polarization would be the major mechanism for causing the large Stokes-shifts of InGaN/GaN MQWs, even with high indium content, where the localization effect is also very strong.

A single (11–22) GaN layer with a thickness of 1.3 $\mu$m is grown on *m*-plane sapphire using our high temperature AlN buffer technique by MOCVD.[14] For the subsequent overgrowth, mask-patterned micro-rod arrays have been fabricated on the semi-polar GaN layer. First, a 500 nm $SiO_2$ layer is deposited by plasma enhanced chemical vapor deposition (PECVD), followed by a standard photolithography patterning process and subsequent dry etching processes using Inductively Reactive Plasma (ICP) and Reactive Ion Etching (RIE) techniques. Regularly arrayed $SiO_2$ micro-rods can be achieved. Finally, the $SiO_2$ micro-rods served as a second mask are used to etch the GaN underneath in order to form regularly arrayed GaN micro-rods with the $SiO_2$ remaining on their top. The micro-rod masks with a diameter of 3.5 $\mu$m have been employed for the fabrication of micro-rod array templates.[13] The subsequent overgrowth process is carried out by MOCVD with a growth temperature, V/III ratio and pressure at 1120 °C, 1600, and 75 Torr, respectively, followed by the growth of InGaN/GaN MQWs. Semi-polar (11–22) InGaN/GaN MQWs with a wide spectral range have been grown, and their peak emission wavelengths span from 497 to 591 nm, covering the whole green and yellow spectral ranges. Detailed X-ray diffraction and transmission electron microscopy (TEM) measurements show the indium composition is from 27% to 47%, demonstrating a great enhancement in indium incorporation over either *c*-plane or non-polar orientation. For comparison, a number of standard *c*-plane InGaN/GaN MQWs samples with indium composition varying from 13% to 32% have also been used for PLE measurements. PLE measurements have been carried out on all the samples loaded in a closed cycle helium cryostat at 12 K. A laser pumped plasma broadband light source with a high density (Energetiq LDLS EQ-99) dispersed by a 320 mm Horiba monochromator is employed as a tunable optical excitation source. The luminescence is dispersed by a 550 mm monochromator and detected by a cooled GaAs photocathode photomultiplier tube (PMT). Time-resolved PL (TRPL) measurements have been performed utilizing a time-correlated single photon counting (TCSPC) technique with a 375 nm pulsed diode laser with a pulse width of 83 ps as an excitation source and a hybrid Hamamatsu PMT as a single photon detector.

As an example, Figure 1 shows PL and PLE spectra from a pair of *c*-plane (polar) and semi-polar (11$\bar{2}$2) InGaN/GaN MQWs samples, both measured at 12 K The PL measurements were carried out with an excitation wavelength of 350 nm, and the PLE measurements have been conducted using their emission peak energies. The two samples show similar peak emission energies located at 2.304 eV (538 nm) and 2.322 eV (534 nm), respectively. The full width at half maximum (FWHM) of the PL spectrum from the semi-polar sample is 187 meV, which is slightly larger than the 166 meV

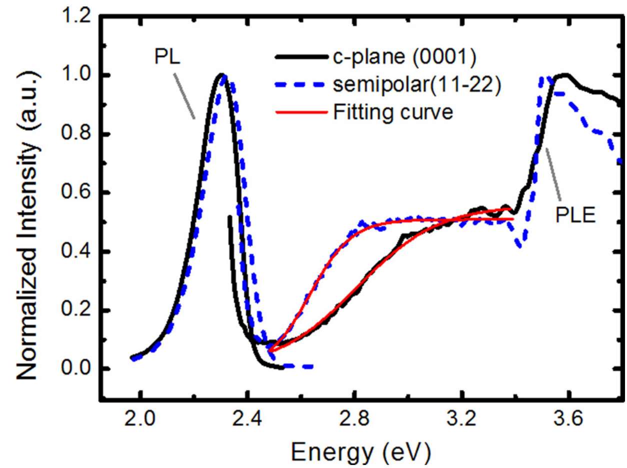


FIG. 1. Low temperature (12 K) PL/PLE spectra of one polar (solid line) and one semi-polar (11$\bar{2}$2) (dashed line) InGaN/GaN MQW samples with emission energy of 2.304 eV (538 nm) and 2.322 eV (534 nm), respectively.

for the *c*-plane sample. The contribution to the PL linewidth broadening as a result of a fluctuation in quantum well thickness can be safely excluded by performing detailed TEM measurements, in which flat quantum wells with a uniform thickness have been demonstrated. Therefore, it is suggested that the broadening of the emission peak in the semi-polar MQWs results from a potential fluctuation caused by an indium segregation within the InGaN quantum wells.[15] Due to the reduced piezoelectric polarization along the semi-polar orientation compared to the *c*-direction, semi-polar InGaN/GaN MQWs require higher indium content than their *c*-plane counterparts in order to achieve a similar emission wavelength. This is expected to lead to stronger localized states in semi-polar MQWs than their *c*-plane counterparts.

PLE measurements were carried out at 12 K with a detection wavelength fixed at each PL peak wavelength. Two absorption edges, associated with the GaN barriers at around 3.43 eV and InGaN quantum wells at the low energy side, respectively, can be seen in both PLE spectra. Comparing the InGaN-related absorption edge in two samples, it is found that the InGaN-related absorption process in the *c*-plane sample covers a wider range of energy (from 3.2 to 2.5 eV) than that in the semi-polar sample (from 2.87 to 2.5 eV), despite the fact that the PL spectrum of the *c*-plane sample is narrower than that of the semi-polar sample. The broadening of the quantum well absorption edge in the *c*-plane sample can be attributed to the quantum confined Franz-Keldysh (QCFK) effects.[16] Due to the internal electric fields, some optical transitions that are normally forbidden may have an chance to become allowed in an absorption process, broadening the quantum well absorption edge.[17] The steep absorption edge in the semi-polar sample is an evidence for the reduced QCFK effects, resulting from the reduced piezoelectric fields in the quantum wells. In order to quantitatively analyze the Stokes shift, the InGaN-related absorption edges can be extracted by fitting with a sigmoidal formula[9]

$$a = a_0 \Big/ \left[1 + \exp\left(\frac{E_B - E}{\Delta E}\right)\right], \quad (1)$$

where $E_B$ is the effective absorption edge; $\Delta E$ is a broadening parameter related to the Urbach tailing energy; and $a_0$ is a constant. The fitted absorption edges are 2.813 eV and 2.634 eV for the *c*-plane and semi-polar samples, respectively. Therefore, the Stokes shift in the *c*-plane sample is 509 meV, which is larger than the 312 meV for the semi-polar sample.

PL and PLE measurements have been carried on a wide range of polar and semi-polar $(11\bar{2}2)$ MQWs samples under the same conditions in order to find a universal rule. The obtained Stokes shift values of the *c*-plane and semi-polar samples as a function of the emission energy are shown in Figure 2. Among these *c*-plane samples, the Stokes shift values linearly decrease with increasing emission energy, and tend to zero at 3.50 eV (i.e., around the GaN bandgap), which is consistent with the previous work reported by other groups.[10] In contrast, all the semi-polar MQW samples show a lower Stokes shift than their *c*-plane counterparts with same emission wavelengths in a wide spectral range of up to yellow. Figure 2 shows a linear relationship between the Stokes shift and the emission energy for both the semi-polar samples and the *c*-plane samples. However, the gradient of the fitting line for the semi-polar samples is smaller than that for the *c*-plane MQWs samples, as denoted beside the fitting lines in Figure 2. Moreover, the fitting line intercepts with the *x*-axis at 3.30 eV, a slight deviation from the GaN bandgap, for which the mechanism is still on investigation.

Since the Stokes shift of InGaN/GaN quantum well structures can be affected by either the piezoelectric field or exciton localization effects or both, low temperature TRPL measurements have been performed on these polar and semi-polar samples in order to further investigate the issue. Due to the QCSE caused by the electric fields across the quantum wells, the probability of optical transitions is reduced. With a widely accepted assumption that non-radiative recombination can be effectively suppressed at a low temperature, such as ~10 K, it is expected that the QCSE leads to an increase in PL decay lifetime. Furthermore, the stronger the QCSE, the longer the recombination lifetime of carriers at a low temperature.

As an example, Figure 3 shows the PL decay traces of two pairs of polar and semi-polar InGaN/GaN MQWs samples with similar emission wavelengths in the green spectral region. The PL decay traces were monitored at their respective emission peak wavelength and can be fitted typically using a bi-exponential equation below:[18]

$$I = A_1 e^{-\frac{t}{\tau_1}} + A_2 e^{-\frac{t}{\tau_2}}, \quad (2)$$

where $\tau_1$ and $\tau_2$ are the decay lifetimes of fast and slow components, respectively; $A_1$ and $A_2$ are constants. The fitting curves are plotted in red lines, and the fast decay lifetimes from the fitting are also denoted beside the curves in Figure 3. As usual a very long lifetime is generally found in the *c*-plane samples, indicating the existence of extremely strong QCSE caused by the internal electric field across the quantum wells. However, the recombination lifetimes of the semi-polar InGaN/GaN MQW samples is approximately one order of magnitude shorter than those observed for the *c*-plane samples, proving a significant decrease in QCSE. A calculation based on a theoretical modelling and analysis made by Brown *et al*. shows that the piezoelectric fields in semi-polar InGaN samples are approximately four times smaller than those in their c-plane counterparts with similar emission wavelengths.[19,20] As the QCSE increases with increasing indium composition in both polar and semi-polar samples, the sample with a longer emission wavelength exhibits a longer PL lifetime, which is true for the *c*-plane samples. For example, the recombination lifetime of the *c*-plane sample ($\lambda = 490$ nm) is 26.7 ns, three times shorter than the 78.4 ns of the *c*-plane sample ($\lambda = 538$ nm). In contrast, for the semi-polar samples, the lifetime changes from 2.7 ns at 497 nm to 3.5 ns at 534 nm, being less sensitive to a change in indium composition compared with the *c*-plane samples. This means that the change of the QCSE with increasing emission wavelength becomes smaller for the semi-polar sample compared with their *c*-plane counterparts,

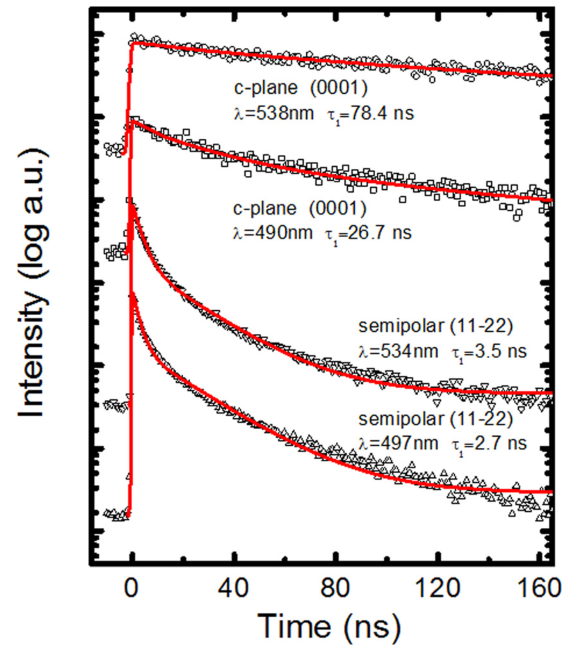


FIG. 3. Decay traces of two polar (0001) and two semi-polar $(11\bar{2}2)$ InGaN/GaN MQW samples with different emission wavelengths measured at 7 K (data are offset for clarity). The dashed lines are the fitting curves with two exponential components model.

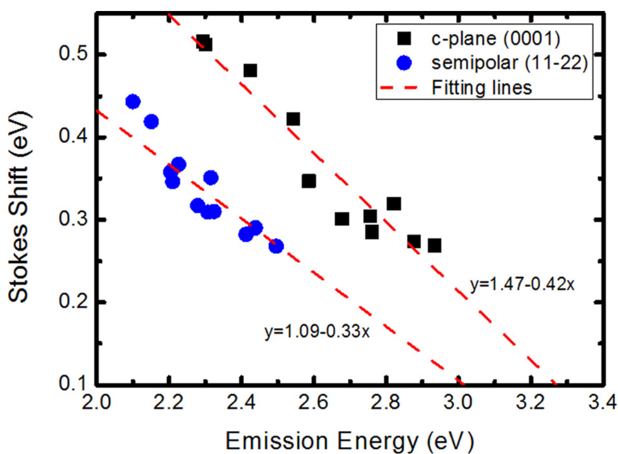


FIG. 2. Stokes Shift as a function of emission energy in polar (0001) and semi-polar $(11\bar{2}2)$ InGaN/GaN MQWs measured at 12 K.

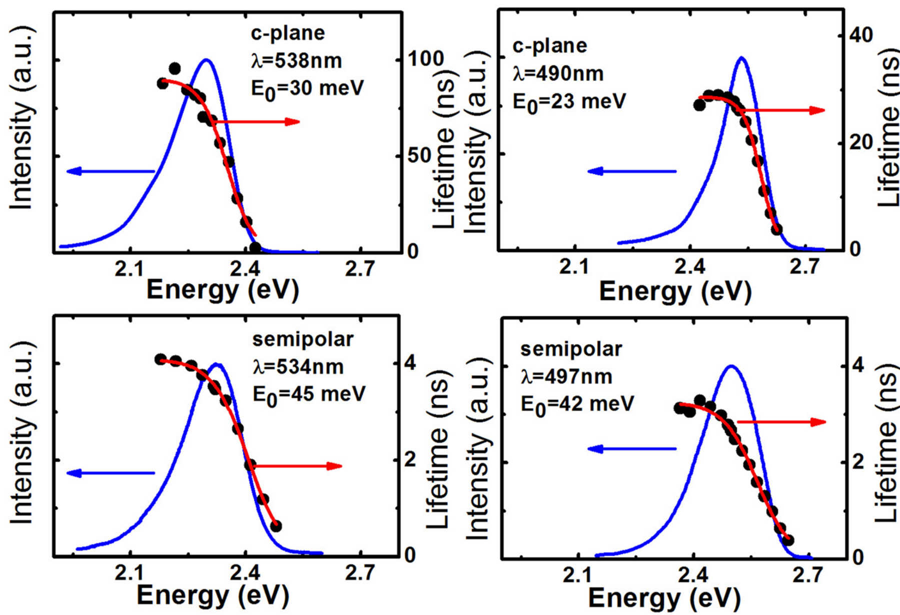


FIG. 4. PL decay time as a function of emission energy for two polar (0001) and two semi-polar ($11\bar{2}2$) InGaN/GaN MQW samples with different emission wavelengths measured at 7 K. The red lines are the fitting results.

which can lead to a reduced slope of the fitting line in Figure 2 if the piezoelectric filed induced polarisation dominates the mechanism for the Stokes shift.

Carrier localization is another major factor which could affect the Stokes shift in InGaN/GaN MQWs. Wavelength-dependent TRPL measurements have been conducted at a low temperature (7 K) to study the localization effects in these samples. Figure 4 presents the fast decay lifetime as a function of the monitored photon energy of the four samples as examples mentioned above. The recombination lifetime decreases with increasing detection energy, indicating the existence of localized excitons in exponential-tail density of states.[21] This can be described by

$$\tau = \tau_{rad} \Big/ \left[1 + \exp\left(\frac{E - E_m}{E_0}\right)\right], \qquad (3)$$

where $\tau_{rad}$ and $E_m$ are the radiative lifetime and the energy of the mobility edge, respectively; $E_0$ represents the exciton localization depth. For the *c*-plane samples, the obtained localization depths are 30 meV and 23 meV for the emission wavelengths at 538 nm and 490 nm, respectively, while the semi-polar samples exhibit localization depths of 45 meV at 534 nm, and 42 meV at 497 nm. Although the Stokes shift values in the semi-polar samples are much smaller than those in the *c*-plane samples, the localization depths in the semi-polar samples are larger than those in the polar samples. This demonstrates that carrier localization effects only contribute a small part to the Stokes shift, compared with the presence of piezoelectric fields.[22] The small Stokes shift for the semi-polar samples results from the significant reduction of the piezoelectric fields. The smaller gradient of fitting line in semi-polar samples results from the fact that the change of the piezoelectric field at different emission wavelengths in semi-polar samples is smaller than that of the *c*-plane samples.

In summary, both PLE and TRPL measurements have been performed on a large number of semi-polar ($11\bar{2}2$) InGaN/GaN MQWs with a wide spectral range of up to yellow grown on our high crystal quality semi-polar GaN, allowing us to systematically investigate the mechanism for the large Stokes shift. Although the semi-polar InGaN/GaN MQWs exhibit larger exciton localization than their *c*-plane counterparts, they display a lower Stokes shift compared with the corresponding *c*-plane counterparts. Furthermore, the Stokes shift values for both the semi-polar samples and their counterparts exhibit a linear relationship with their emission energy, but the semi-polar samples with a reduced gradient. All these demonstrate that the piezoelectric field induced polarization is the major mechanism for causing the large Stoke shift.

This work was supported by the UK Engineering and Physical Sciences Research Council (EPSRC) and Seren Photonics Ltd. in the UK.

[1]F. Scholz, Semicond. Sci. Technol. **27**, 024002 (2012).
[2]I. Ho and G. Stringfellow, Appl. Phys. Lett. **69**, 2701 (1996).
[3]M. Beeler, E. Trichas, and E. Monroy, Semicond. Sci. Technol. **28**, 074022 (2013).
[4]J. E. Northrup, Appl. Phys. Lett. **95**, 133107 (2009).
[5]H. C. Yang, P. F. Kuo, T. Y. Lin, Y. F. Chen, K. H. Chen, L. C. Chen, and J.-I. Chyi, Appl. Phys. Lett. **76**, 3712 (2000).
[6]H.-S. Kwack, B.-J. Kwon, J.-S. Chung, Y.-H. Cho, S.-Y. Kwon, H. J. Kim, and E. Yoon, Appl. Phys. Lett. **93**, 161905 (2008).
[7]Y. H. Cho, J. J. Song, S. Keller, M. S. Minsky, E. Hu, U. K. Mishra, and S. P. DenBaars, Appl. Phys. Lett. **73**, 1128 (1998).
[8]Z. C. Feng, L.-H. Zhu, T.-W. Kuo, C.-Y. Wu, H.-L. Tsai, B.-L. Liu, and J.-R. Yang, Thin Solid Films **529**, 269 (2013).
[9]K. P. O'Donnell, R. W. Martin, and P. G. Middleton, Phys. Rev. Lett. **82**, 237 (1999).
[10]R. W. Martin, P. G. Middleton, K. P. O'Donnell, and W. Van der Stricht, Appl. Phys. Lett. **74**, 263 (1999).
[11]K. Xing, Y. Gong, J. Bai, and T. Wang, Appl. Phys. Lett. **99**, 181907 (2011).
[12]J. Bai, Y. Gong, K. Xing, X. Yu, and T. Wang, Appl. Phys. Lett. **102**, 101906 (2013).
[13]Y. Gong, K. Xing, B. Xu, X. Yu, Z. Li, J. Bai, and T. Wang, ECS Trans. **66**, 151 (2015).
[14]T. Wang, K. B. Lee, J. Bai, P. J. Parbrook, R. J. Airey, Q. Wang, G. Hill, F. Ranalli, and A. G. Cullis, Appl. Phys. Lett. **89**, 081126 (2006).
[15]N. P. Hylton, P. Dawson, C. F. Johnston, M. J. Kappers, J. L. Hollander, C. McAleese, and C. J. Humphreys, Phys. Status Solidi C **6**, S727 (2009).

[16]S. F. Chichibu, A. C. Abare, M. S. Minsky, S. Keller, S. B. Fleischer, J. E. Bowers, E. Hu, U. K. Mishra, L. A. Coldren, S. P. DenBaars, and T. Sota, Appl. Phys. Lett. **73**, 2006 (1998).
[17]D. A. B. Miller, D. S. Chemla, and S. Schmitt-Rink, Phys. Rev. B **33**, 6976 (1986).
[18]S. F. Chichibu, K. Hazu, Y. Ishikawa, M. Tashiro, H. Namita, S. Nagao, K. Fujito, and A. Uedono, J. Appl. Phys. **111**, 103518 (2012).
[19]W. Chow, M. Kira, and S. W. Koch, Phys, Rev. B **60**, 1947 (1999).
[20]I. H. Brown, P. Blood, P. M. Smowton, J. D. Thomson, S. M. Olaizola, A. M. Fox, P. J. Parbrook, and W. W. Chow, IEEE J. Quantum Electron. **42**, 1202 (2006).
[21]S. F. Chichibu, T. Azuhata, H. Okumura, A. Tackeuchi, T. Sota, and T. Mukai, Appl. Surf. Sci. **190**, 330 (2002).
[22]E. Berkowicz, D. Gershoni, G. Bahir, E. Lakin, D. Shilo, E. Zolotoyabko, A. C. Abare, S. P. DenBaars, and L. A. Coldren, Phys. Rev. B **61**, 10994 (2000).